Cysteine Scanning Mutagenesis of TM5 Reveals Conformational Changes in OxlT, the Oxalate Transporter of *Oxalobacter formigenes*†

Xicheng Wang, Liwen Ye, Caleb C. McKinney, Mingye Feng, and Peter C. Maloney*

Department of Physiology, Johns Hopkins Medical School, Baltimore, Maryland 21205

Received January 23, 2008; Revised Manuscript Received April 1, 2008

ABSTRACT: We constructed a single-cysteine panel encompassing TM5 of the oxalate transporter, OxlT. The 25 positions encompassed by TM5 were largely tolerant of mutagenesis, and functional product was recovered for 21 of the derived variants. For these derivatives, thiol-directed MTS-linked agents (MTSEA, MTSCE, and MTSES) were used as probes of transporter function, yielding 11 mutants that responded to probe treatment, as indicated by effects on oxalate transport. Further study identified three biochemical phenotypes among these responders. Group 1 included seven mutants, exemplified by G151C, displaying substrate protection against probe inhibition. Group 2 was comprised of a single mutant, P156C, which had unexpected behavior. In this case, we observed increased activity if weak acid/base or neutral probes were used, while exposure to probes introducing a fixed charge led to decreased function. In both instances, the presence of substrate prevented the observed response. Group 3 contained three mutants (e.g., S143C) in which probe sensitivity was increased by the presence of substrate. The finding of substrate-protectable probe modification in groups 1 and 2 suggests that TM5 lies on the permeation pathway, as do its structural counterparts, TM2, TM8, and TM11. In addition, we speculate that substrate binding facilitates TM5 conformational changes that allow new regions to become accessible to MTS-linked probes (group 3). These biochemical data are consistent with the recently developed OxlT homology model.

The membrane transporter OxlT is found in *Oxalobacter formigenes*, a Gram-negative anaerobe that resides in the mammalian intestine (*1*). In *O. formigenes*, OxlT mediates the heterologous exchange of external oxalate^{2-} and internal formate^{-}, the product of oxalate decarboxylation (*1, 2*). The phenomenological coupling between the vectorial and scalar reactions leads to generation of a proton-motive force that drives ATP synthesis and other membrane activities (*2, 3*). Subsequent work has indicated that this organizational scheme is found in a large number of other microbes, both Gram-negative and Gram-positive (*4*).

Bioinformatic analysis shows that OxlT belongs to the major facilitator superfamily (MSF)[1] (*5*), the largest collection of secondary carrier-type transporters. It is also apparent that while individual members of MFS may exhibit a broad range of substrate specificity, including sugars, antibiotics, and neurotransmitters, as a group they share an architectural theme in which a central loop of variable size connects a pair of domains, each of which usually contains six transmembrane helices (TM_{1-6} and TM_{7-12}). A form of the MFS signature sequence is typically found at the cytoplasmic end of TM2 (GX_3[D/E][R/K]XG[R/K]R/K]) and in some cases is replicated at the cytoplasmic end of TM8, as in OxlT and GlpT (*5–7*).

New insight into structure−function relationships within the MFS has been offered by crystal structures obtained for four separate examples. Initially, a 6.5 Å resolution structure of OxlT, obtained by electron crystallography, established the general features of helix organization, symmetry, and connectivity within the MSF (*8, 9*). More detailed views of individual cases followed from X-ray crystallography of the H^+/lactose symporter (LacY), the phosphate/glycerol 3-phosphate antiporter (GlpT), and the H^+/drug antiporter (EmrD) (*10–12*). These latter findings prompted derivation of an OxlT homology model, using the GlpT X-ray structure as a template (*13*). This, in turn, has led to new biochemical experiments that strengthened a mechanistic view of OxlT function (*13, 14*).

In the low-resolution electron crystallographic map of OxlT (*8, 9*), as well as in the OxlT homology model (*13*), the molecule is composed of four sequential three-helix units, TM_{1-3}, TM_{4-6}, TM_{7-9}, and TM_{10-12}, in which the individual units are paired so that the permeation pathway is defined by the interface of two larger domains, TM_{1-6} and TM_{7-12}. Earlier study implicated TM2, TM8, and TM11 as containing residues directly associated with substrate transport by OxlT (*13–17*). In particular, two substrate-binding elements (R272 and K355) are found on TM8 and TM11, respectively (*13–15*), while residues on TM2 (Q63) and TM11 (S359) are known to lie on the permeation pathway (*15–17*). These observations are consistent with the OxlT structural model,

† This work was supported by National Institutes of Health Grant GM24195.

* To whom correspondence should be addressed: Department of Physiology, Johns Hopkins Medical School, Baltimore, MD 21205. Telephone: (410) 955-8325. Fax: (410) 614-8331. E-mail: pmaloney@jhmi.edu.

[1] Abbreviations: DMSO, dimethyl sulfoxide; MFS, major facilitator superfamily; MTS, methanethiosulfonate; MTSCE, carboxyethyl methanethiosulfonate; MTSEA, methanethiosulfonate ethylamine; MTSES, methanethiosulfonate ethylsulfonic acid; MTSET, methanethiosulfonate ethyltrimethylamine; MTSHE, hydroxyethyl methanethiosulfonate; MTSMT, methanethiosulfonate methyltrimethylamine; MTSPA, methanethiosulfonate propylamine; TM, transmembrane helix.

10.1021/bi8001314 CCC: $40.75
Published on Web 05/02/2008

which suggests that four helices (TM2, TM5, TM8, and TM11), one from each of the four three-helix units, form portions of the wall surrounding the transport pathway (see ref *13*). For these reasons, examination of TM5, which has not yet been experimentally probed, seemed an attractive candidate for further the study of structure−function relationships in OxlT.

The work summarized here was designed to address the issue of whether TM5 lies on the permeation pathway, as do its symmetry-related counterparts, TM2, TM8, and TM11. Our study provides an affirmative answer to this question. Unexpectedly, our findings also provide evidence suggesting that TM5 is involved in protein conformational changes induced by substrate binding and/or transport.

EXPERIMENTAL PROCEDURES

Mutagenesis and Protein Expression. OxlT and its mutants were encoded within a 1.4 kb XbaI−HindIII fragment in pBluescript II SK$^+$ (*18, 19*). To suppress uninduced protein expression, the Amp^r plasmid harboring OxlT was carried in *Escherichia coli* strain XL1 together with plasmid pMS421 (Spec^r, LacI^q) (*18*). A cysteine-less variant of OxlT (C28G/C271A) carrying a C-terminal polyhistidine (His_9) tail (*19*) was used as a parent to all single-cysteine mutations; this derivative is fully functional, with kinetic properties comparable to those of wild-type OxlT (*15*). All variants were acquired by Cameleon or QuikChange mutagenesis (Stratagene) and confirmed by DNA sequencing. For protein expression, a single colony from a fresh transformation was placed in LB broth containing antibiotics and grown overnight at 35 °C. Cells from the overnight growth were diluted 100-fold into fresh medium and grown with shaking at 35 °C until A_{600} reached 0.12, at which point OxlT expression was induced by addition of 1 mM IPTG. Cells were harvested after an additional 3 h. To detect OxlT in crude detergent extracts or after reconstitution into proteoliposomes, immunoblots were probed with antibody directed against polyhistidine, and chemilumenescence was monitored using a Fuji LAS1000 gel documentation system (*16*). With few exceptions (noted in Results), mutants were expressed at levels satisfactory for functional analysis (≥20% of the parental level).

Reconstitution and Assays of OxlT Function. Membranes prepared by osmotic lysis (*18, 19*) were solubilized in buffer containing 100 mM potassium oxalate, 50 mM potassium phosphate (pH 7), 20% (v/v) glycerol, 1.5% (w/v) octyl glucoside, and 0.5% (w/v) *E. coli* phospholipid (stored under nitrogen after hydration in distilled water). The protease inhibitor 4-(2-aminoethyl)benzenesulfonyl fluoride was normally present at 0.25 mM. Purified protein (0.9−1.8 mg/mL) was obtained by metal-chelate affinity chromatography as described previously (*14, 15*), with final elution at pH 4.3 using 100 mM potassium oxalate, 50 mM potassium acetate, 20% glycerol, 0.1% (w/v) *E. coli* phospholipid, and 0.25% (w/v) diheptanoylphosphatidylcholine (*8, 14*). Crude detergent extracts and purified proteins were reconstituted by detergent dilution (*13, 18, 20*), using a method adapted from earlier work (*21–23*), to give proteoliposomes loaded with 100 mM potassium oxalate and 50 mM potassium phosphate (pH 7).

We elected to monitor OxlT function by tests of oxalate transport, since the alternate substrate, formate, has a relatively low affinity (*2, 14*). In routine experiments, [^{14}C]-oxalate transport was assessed at room temperature by a rapid filtration assay (*13*). Duplicate 0.2 mL aliquots of the proteoliposome suspension were directly spotted onto filter paper discs and washed twice with cold assay buffer [100 mM potassium sulfate and 50 mM potassium phosphate (pH 7)], and after the vacuum had been disengaged, proteoliposomes were overlaid with 0.2 mL of assay buffer containing 100 μM [^{14}C]oxalate. The reaction was terminated after 50 s by reinstituting vacuum filtration, with washing as described above.

In kinetic studies of single-cysteine variants, a conventional "tube" assay was used for better time resolution (*13*). After reconstitution, proteoliposomes were washed twice with iced assay buffer by centrifugation in a Beckman Optima ultracentrifuge (140000*g* for 30 min) and finally resuspended as a concentrated stock in the same buffer. Duplicate aliquots of the stock were then diluted 10-fold into assay buffer at room temperature, after which labeled substrate was added at known concentrations; after 40 s, the reaction was quenched by filtration and washing to estimate initial rates of [^{14}C]oxalate self-exchange.

Treatment with MTS-Linked Probes. To identify and characterize inhibition of single-cysteine mutants by MTS-linked probes (*14, 16, 17*), duplicate samples of the proteoliposome suspension trapped on a Millipore filter (see above) were washed twice with assay buffer and then overlaid for 7 min at room temperature with 0.3 mL of assay buffer containing MTSEA, MTSCE, or MTSES at the desired concentration. Probes were prepared as stocks (usually, 1 M) in dimethyl sulfoxide, and solvent-treated preparations served as controls. After being exposed to the probe, proteoliposomes were rinsed twice with 5 mL of assay buffer, and OxlT function was assessed, using a second, 40 s overlay with 0.2 mL of 100 μM [^{14}C]oxalate. When protection by substrate was studied, the incubation with probe was carried out in the presence of increasing concentrations of potassium oxalate (from 0 to 100 mM), together with compensatory decreases in the level of potassium sulfate in the assay buffer (from 100 to 0 mM). Responses to substrate protection were fit to a simple kinetic model developed earlier to analyze substrate protection of cysteine substitutions in TM2 and TM11 (*16, 17*). The model assumes that unliganded OxlT reacts with either substrate or probe to generate either liganded OxlT or an irreversibly inhibited complex, respectively. If only the unliganded OxlT can be modified by the probe, the fraction of the OxlT population that remains unmodified (F) and the dissociation constant of the substrate−OxlT complex (K_D) are related by

$$\ln(F) = -kPt/(1 + S/K_D)$$

where S and P represent substrate and probe concentrations, respectively, t is time, and k is the rate constant describing probe modification.

RESULTS

TM5 Single-Cysteine Substitutions. The OxlT homology model suggests that TM5 contains 25 residues (G140−V164) (*13*). Accordingly, we constructed a single-cysteine panel

Table 1: TM5 Single-Cysteine Mutants

	relative specific activity[a] (%)		relative specific activity[a] (%)
GA	100	L152C	51
G140C	≤1	G153C	–[b]
L141C	92	V154C	39
A142C	107	L155C	72
S143C	84	P156C	30
G144C	≤1	F157C	57
F145C	113	L158C	60
T146C	112	P159C	77
A147C	25	L160C	79
A148C	92	I161C	59
G149C	10	S162C	65
Y150C	≤1	S163C	59
G151C	51	V164C	37

[a] Specific activity is given relative to the C28G/C271A cysteine-less parental protein (GA); data reflect mean values from duplicate measurements. [b] Mutant protein not expressed.

of mutants in this region and evaluated OxlT function for each mutant relative to the cysteine-less parental protein (Table 1). Among this group, 21 single-cysteine variants retained specific activities between 10 and 110% of that found for the parental protein, suggesting that the introduction of cysteine at most positions in TM5 did not irreversibly perturb OxlT function. Three mutants exhibited relative specific activities of ≤1% (G140C, G144C, and Y150C), while one mutant was not expressed (G153C); these four variants were not studied further.

Response to MTS-Linked Probes. To identify TM5 residues of possible functional significance, the 21 active single-cysteine mutants (Table 1) were individually reconstituted into liposomes and exposed to excess (2 mM) MTS-linked agents that introduced one of three kinds of thiol modification: MTSCE and MTSEA, which yield weak acidic ($-SCH_2CH_2COOH$) or basic ($-SCH_2CH_2NH_2$) functions, respectively, and MTSES, which implants a permanent anionic charge ($-SCH_2CH_2SO_3^-$). For the 11 mutants responding to such treatment, we assumed that any observed effect reflected covalent modification of the targeted cysteine, as confirmed by mass spectrometry in earlier examples (*14*). In this survey, all but one of the 11 affected variants exhibited significant inhibition after probe treatment (Figure 1). Near-complete inhibition (≥90−95%) by one or more probes was recorded in seven mutants (A142C, S143C, A147C, G151C, L152C, V154C, and L161C), while three others (L155C, F157C, and L158C) exhibited a clear but less pronounced response (ca. 80% inhibition). Previous work (*16*) showed that after its reconstitution, OxlT is found in proteoliposomes in both right-side-out and inside-out orientations, in approximately equal proportions. Since the mutants inhibited by MTS-linked probes mutants were 80% blocked by at least one MTS-linked probe, it seemed likely that probe(s) reactivity with the target cysteines has no strong preference for either orientation. This is in line with other observations with both OxlT (*16*) and UhpT (*24, 25*), where no evidence of orientation-specific responses to such probes was found.

In one case, P156C, the results of MTS modification were unusual. Preliminary screens gave mixed results; that is, 2−3-fold increased activity was found after treatment with excess MTSEA or MTSCE, but marked inhibition followed exposure to MTSES. Additional tests confirmed and amplified these findings. In these latter cases, together with the agents described above, we selected MTS-linked probes introducing a neutral group, such as MTSHE ($-SCH_2CH_2OH$), a more extended amino function, as in MTSPA ($-SCH_2CH_2CH_2NH_2$), and MTSMT or MTSET, each of which introduces a fixed positive charge [$-SCH_2N(CH_3)_3^+$ or $-SCH_2CH_2CN(CH_3)_3^+$, respectively]. The diversity of responses by P156C seen earlier was confirmed by this wider study (Figure 2). Thus, probes that would implant a permanent fixed charge (MTSES, MTSMT, and MTSET) gave clear inhibition (40−60%), yet marked enhancement (as much as 3-fold, restoring the parental level) was observed for probes that introduce an uncharged adduct (MTSHE) or a modification whose weakly acidic or basic character suggests it might exist in an uncharged form (MTSEA, MTSPA, and MTSCE). Added mutagenesis of P156 was largely consistent with these findings. Thus, nonfunctional product was found for the P156D, P156K, and P156R derivatives, while other mutants (P156G, P156A, P156L, P156S, and P156H) exhibited residual specific activities of 20−65% relative to the parent, cysteine-less protein. Taken together, these findings suggest that as such, P156 is not essential for OxlT function but that the environment surrounding the side chain should retain a nonpolar character. This is consistent with the presumed location of P156, deep within the permeation pathway in the inward-facing conformation (ref *13*, and see below).

In more detailed work, we characterized the kinetic parameters of the mutants responding to MTS modification, as well as an estimate of their sensitivity to MTSCE (Table 2). It appeared that cysteine replacement had its major impact as a reduction of maximal velocity, with a relatively modest effect (usually, ≤2-fold) on the measured Michaelis constant (K_M) for oxalate transport. The exception to this is the V154C mutant, where the major impact of substitution mutagenesis was on the K_M. In other work, we found that sensitivity to MTSCE varied over a 100-fold range, including four positions of relatively high accessibility (IC_{50} of 40−100 μM), two of moderate sensitivity (IC_{50} of 200−300 μM), and four that responded to only relatively high levels of the probe ($IC_{50} \geq 1000-4000$ μM).

Substrate Protection. The permeation pathway may be defined as the collection of residues exposed to the hydrophilic environment in the inward- and outward-facing conformations of the transporter (*25*), and cysteine scanning mutagenesis has been used to develop two operational tools useful in characterizing such positions (*14, 16, 17, 25, 26*). For example, one expects that cysteine substitutions in such residues may provide informative targets for hydrophilic, thiol-directed probes able to enter the pathway and that this can occur, in principle, for probes entering from either end of the pathway (*25, 14, 16, 17*). Second, one also anticipates that if substrate is present, probe modification may be affected. Thus, binding of substrate may physically block access to the target cysteine, conformational changes accompanying substrate binding may alter the likelihood of probe access, or the initiation of turnover may shift the distribution of kinetic species to favor or disfavor those that are sensitive to probe modification. In this work, use of MTS-linked agents identified 11 TM5 single-cysteine mutants that were substantially affected by probe treatment. Accordingly, for this set, added tests were conducted to examine whether substrate had significant effects on probe modification as

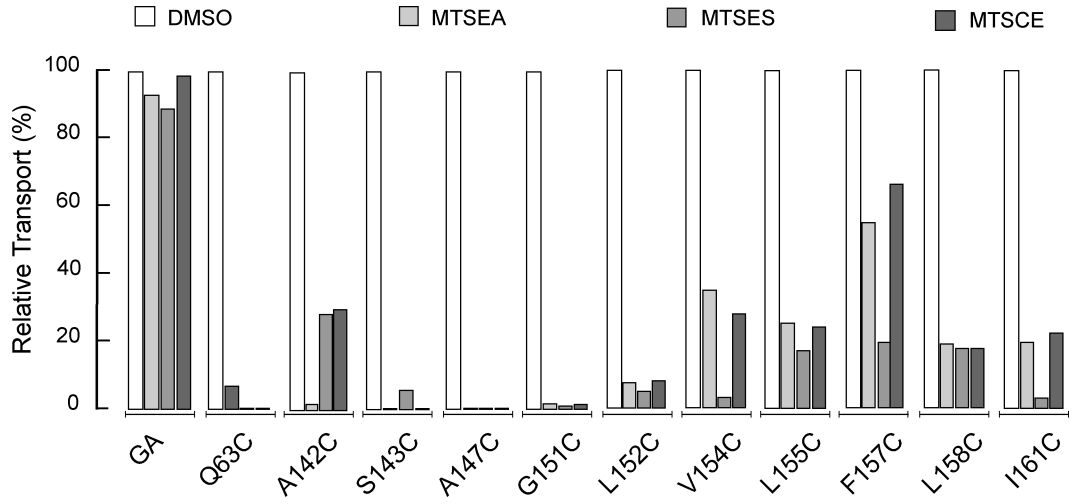

FIGURE 1: Sensitivity of TM5 single-cysteine mutants to MTS-linked probes. Twenty-one TM5 single-cysteine mutants (see Table 1) were reconstituted into proteoliposomes to examine their responses to MTS-linked probes; the parental cysteine-less parent (GA) and a single-cysteine mutant in TM2 (Q63C) of known probe sensitivity (*16*) served as negative and positive controls, respectively. Proteoliposomes were exposed for 7 min to excess (2 mM) MTSEA, MTSES, and MTSCE from concentrated stocks in DMSO, and after the probe had been removed, [^{14}C]oxalate self-exchange, relative to the DMSO-treated control, was measured in duplicate samples. Ten mutants displayed significant (≥80%) inhibition by at least one probe, as indicated. One mutant (P156C) showed a complex response and is presented separately (see below). All other mutants showed no response relative to the DMSO-treated control (±15% change) and have been omitted. Data are mean values from duplicate trials.

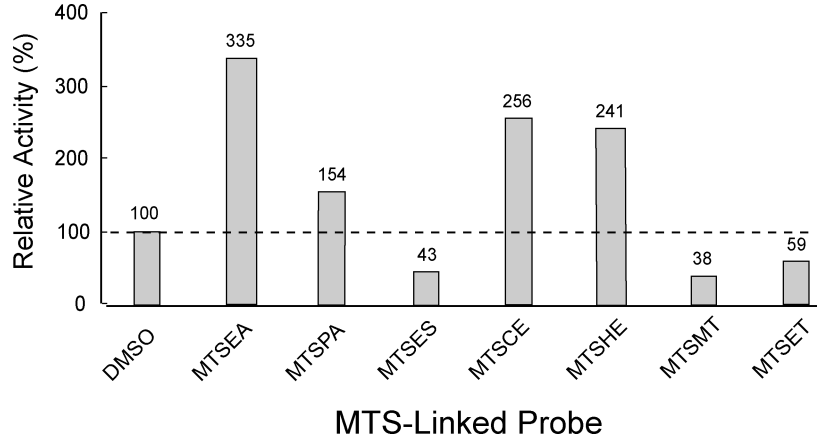

FIGURE 2: Response of P156C to MTS-linked probes. Proteoliposomes containing the P156C derivative were exposed to excess MTS-linked probes as described in the legend of Figure 1. [^{14}C]Oxalate self-exchange was assessed in duplicate samples and is given relative to the DMSO-treated control. The following MTS-linked probes were used: MTSEA, MTSPA, MTSES, MTSCE, MTSHE, MTSMT, and MTSET.

Table 2: Kinetic Analysis of MTSCE-Sensitive Residues

sample[a]	K_M (μM)	V_{max} (μmol min^{-1} mg^{-1})	IC_{50}[b] (μM MTSCE)
GA	110	2300	>5000
A142C	180	1400	1500
S143C	170	1000	90
A147C	115	400	60
G151C	150	1600	100
L152C	130	1800	40
V154C	490	1900	2000
L155C	240	1500	1000
P156C	86	200	see the text
F157C	260	1400	4000
L158C	210	1000	200
I161C	180	300	300

[a] Kinetic analysis of the C28G/C271A cysteine-less parent (GA) and the indicated single-cysteine derivatives was performed as described in Experimental Procedures. [b] IC_{50}, the MTSCE concentration giving 50% inhibition of [^{14}C]oxalate self-exchange after a 7 min treatment of proteoliposomes prior to the assay (see Experimental Procedures).

judged by changes in specific activity. This information allowed us to place the 11 variants in three distinct groups.

Group 1 includes seven mutants (G151C, L152C, V154C, L155C, F157C, L158C, and I161C) that were inhibited by MTS-linked agents and whose inhibition could be prevented by the presence of substrate. In most cases, we used excess probe to maximize inhibition, and for this condition, co-incubation with 100 mM oxalate (potassium salt) was sufficient to fully protect most mutant proteins; in two instances (L158C and I161C), however, probe concentration had to be lowered to achieve 60−70% inhibition before significant protective effects (≥80% rescued) were observed. Group 2 includes only one example, P156C. While P156C itself has a complex set of responses to different MTS-linked agents (Figure 2 and text), co-incubation of probe and substrate blocked the effect of modification. Thus, whether the probe led to increased or decreased P156C function, no effect was seen if substrate (100 mM oxalate) is present along with probe. Therefore, in principle, both members of group 1 and group 2 satisfied the two criteria noted above, providing evidence that these eight positions may be on the permeation

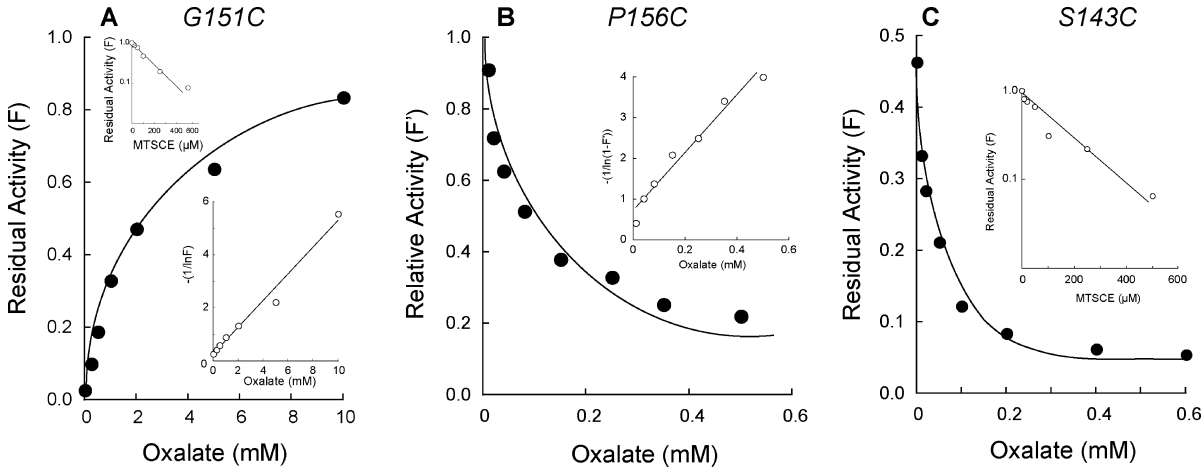

FIGURE 3: Effects of oxalate on the response to MTSCE by single-cysteine variants representing groups 1−3. (A) G151C (group 1). Duplicate samples of proteoliposomes were treated for 7 min with 1 mM MTSCE in assay buffer, or assay buffer containing the indicated concentrations of oxalate. After the reaction had been quenched, initial rates of [^{14}C]oxalate self-exchange were measured; residual activity is shown relative to samples not exposed to MTSCE. In the insets, (top) titration with MTSCE yielded an IC_{50} of 100 μM and (bottom) a linear transform of substrate-dependent protection was used to extract the apparent K_D for oxalate protection (see Experimental Procedures). (B) P156C (group 2). Duplicate samples of proteoliposomes containing the P156C variant were exposed to excess 5 mM MTSCE to achieve ca. 250% stimulation (see Figure 2); parallel samples were exposed to 5 mM MTSCE in the presence of oxalate at the indicated concentrations. Residual activity is given relative to that found with MTSCE alone. In the inset, a linear transform modified from that described for panel A (see Experimental Procedures) was used to estimate the K_D for oxalate as an inhibitor of enhancement arising from MTSCE treatment: $\ln(1 - F') = -kPt/(1 + S/K_D)$, where $1 - F'$ represents the observed enhancement relative to that found without substrate; other symbols are as given before (see Experimental Procedures). (C) S143C (group 3). Duplicate samples of proteoliposomes were treated with 100 μM MTSCE to achieve near-50% residual activity. In parallel samples, 100 μM MTSCE was used in the presence of oxalate at the indicated concentrations. [^{14}C]Oxalate self-exchange is shown relative to that found with MTSCE alone. In the inset, titration with MTSCE in the absence of substrate was used to determine an approximate IC_{50} of 120 μM.

pathway. Group 3 is comprised of three mutants (A142C, S143C, and A147C). In these cases, initial trials assessing the effects of substrate were unsuccessful. Further tests, at lower levels of the probe, revealed an unexpected response for all three mutants. Rather than protection from the effects of probe, the presence of substrate increased the efficiency of probe inhibition.

Residues on the Permeation Pathway. From each of these groups, we selected one mutant to perform more detailed quantitative assays, using both MTSCE and MTSES. Since the findings with MTSCE or MTSES modification were similar, we present only data from trials using MTSCE.

In group 1, dose-dependent inhibitions of G151C were used to determine an MTSCE concentration suitable for quantitative study. In this case, titration with MTSCE showed that 50% inhibition was given by 100 μM MTSCE (Table 2) for our usual conditions of treatment (7 min). For these same conditions, we exposed G151C to excess MTSCE (2 mM) in the presence of an increasing level of potassium oxalate. With no addition of substrate, inhibition by MTSCE was virtually complete (≥98%), but in the presence of increasing concentrations of substrate, inhibition was progressively relieved; ca. 80% protection was afforded with 10 mM oxalate (Figure 3A). The substrate dependence of this protection could be fit to a simple kinetic model developed earlier for analyzing comparable effects of MTSCE and MTSES in TM2 and TM5 (*16, 17*) (see Experimental Procedures). In this case, the derived K_D value for substrate production was 0.7 mM, close to the K_M for oxalate transport by G151C (0.2 mM) (Figure 3A, inset, and Table 2).

In group 2, comprised solely of P156C, modification by MTSCE served to enhance function (Figure 2). This response appeared to saturate near 10 mM MTSCE (not shown), but a significant functional increase was retained at the moderate concentration we chose to examine in detail (5 mM MTSCE) (Figure 3B). As with the G151C variant, we observed that the response of P156C to MTSCE modification progressively diminished as the substrate concentration increased (Figure 3B), with a nearly complete absence of effect when oxalate was present at 0.5 mM. Since MTSCE increased P156C transport activity, we modified the analysis used above for deriving K_D by considering only the positive increment as reflecting modification by probe. This led us to estimate a derived K_D value of ca. 0.1 mM for "protection" of P156C against MTSCE (Figure 3B, inset). We also assessed the kinetic behavior of P156C and MTSCE-modified P156C to determine the origin of enhanced activity. These experiments (not given) showed that the K_M of the modified protein was essentially unchanged from that measured earlier [0.24 mM (Table 2)], with increased activity attributable wholly to an elevated maximal velocity.

Conformational Changes in TM5. For analysis of MTSCE inhibition of S143C, a member of group 3, we first explored its response to a range of MTSCE concentrations. Thus, for the standard exposure time of 7 min, we recorded a first-order decay (as for G151C) with a 50% inhibition near 120 μM MTSCE (Figure 3C, inset), comparable to the value (90 μM) obtained earlier (Table 2). In a parallel experiment, a residual 45% activity after treatment with 100 μM MTSCE was set as a baseline for the subsequent test of substrate effects. As expected, the efficiency of MTSCE inhibition was increased as a function of added substrate, with nearly complete inhibition (ca. 95%) as the oxalate concentration increased above 0.5 mM (Figure 3C). Evidently, a protein conformational change was induced by the presence of substrate, placing S143C in a position more readily attacked by added probe.

Table 3: Substrate-Induced MTSCE Sensitivity in P156 and P159 Mutants

variant[a]	[MTSCE] (μM)	residual activity (%)[b]	
		without oxalate	with 5mM oxalate
G151C	2000	6	87
G151C/P156L	2000	4	66
G151C/P159A	2000	4	65
S143C	90	43	7
S143C/P156L	20	46	47
S143C/P159A	200	43	23

[a] Assay of [^{14}C]oxalate self-exchange (as in Table 1) showed that the specific activities of the A151C/P156L and A151C/P159C double mutants were 17 and 43%, respectively, of that of the cysteine-less parent; the specific activities of the S143C/P156L and S143C/P159A derivatives were 14 and 40%, respectively. [b] Activity relative to the DMSO-treated control. MTSCE was provided at the indicated concentration in the presence or absence of 5 mM oxalate. Note that excess MTSCE was used to inhibit G151C and its derivatives, while MTSCE approximating an IC_{50} was used for S143C and its derivatives.

In the OxlT homology model (*13*), the central region of TM5 contains two proline residues (P156 and P159), one of which (P156) is associated with a kink in the helical character of TM5. Others have suggested that in transport proteins, the presence of proline in the hydrophobic sector may be related to dynamical behavior (*27, 28*), and this idea prompted us to ask whether the unexpected behavior of group 3 residues (Figure 3C) was influenced by either (or both) P156 or P159. To address the question, we screened several mutants at positions 156 and 159 and chose for further study the P156L and P159A derivatives (specific activities of 55 and 78% of that of their cysteine-less parent, respectively). In turn, these mutants were recipients of the G151C mutation, which served as a neutral control, or the test mutation, S143C. As anticipated, the responses of the double mutants containing G151C mirrored that of the G151C single mutant; that is, treatment with 2 mM MTSCE alone gave a substantial inhibition (ca. 95%) that was largely prevented in the presence of substrate (Table 3). More interestingly, in the double mutants containing S143C, mutation of P156 eliminated the substrate-induced increase in sensitivity found in the parental protein, yet this behavior was retained in the absence of P159. To further differentiate the impact of P156 and P159 on substrate-triggered accessibility, we also monitored the response to MTSCE with and without excess substrate (5 mM) over a range of probe concentrations, for S143C alone and for the double mutants combining it with P156L or P159A (Figure 4). For the S143C single mutant, the response to MTSCE was consistent with earlier work (Figure 3 and Table 3), in that the presence of substrate enhanced the efficiency of MTSCE inhibition (ca. 6-fold). A comparable enhancement (ca. 5-fold) was found in the double mutant eliminating P159 (S143C/P159A), but no substrate effect was elicited in the mutant lacking P156. These data clearly implicate P156 as being instrumental in mediating substrate-triggered probe sensitivity of group 3 residues.

DISCUSSION

The OxlT homology model (*13*) is consistent with previous biochemical studies that used functional tests to identify residues TM2, TM8, and TM11 as being within the permeation pathway (*14, 16, 17*). The success of this model likely relates to both structural and functional similarities between OxlT and GlpT, the structure of which (*8*) provided the template for model building. Thus, both proteins are within the MFS and share the same overall helix organization, and in both cases, ligand binding occurs near the center of the pathway by means of ionic interaction between a pair of positively charged residues and the divalent substrate anion (*8, 13, 14, 29*). Nevertheless, GlpT and OxlT exhibit important structural differences. In particular, while in GlpT the substrate-binding elements (R46 and R269) are found at equivalent positions on TM1 and TM7 within the homologous N-terminal (TM_{1-6}) and C-terminal (TM_{7-12}) domains (*8*), the main ligand-binding residues of OxlT lie wholly in the C-terminal domain, on TM8 (R272) and TM11 (K355) (*13, 14*). This distinction has mechanistic implications. Thus, in the "rocker-switch" model proposed for GlpT (*8, 30, 31*), the long central loop connecting TM6 and TM7 enables rotation of the N- and C-terminal domains against each other along an interface compromised of two helical pairs, TM2−TM11 and TM5−TM8. This conformational change is thought to be triggered by ligand binding, since substrate is in direct contact with residues on either domain. In OxlT, however, the finding that the primary substrate-binding residues do not bridge these two domains raises the possibility that the GlpT rocker-switch mechanism might not apply. In this setting, then, we sought to study TM5 to determine if residues on TM5 lie on the permeation pathway, as do residues in its symmetry-related partners, TM2, TM8, and TM11 (Figure 5A). Unexpectedly, we also obtained evidence bearing on the more general question of the role of the OxlT N-terminal domain (TM_{1-6}) and the relevance of the rocker-switch mechanism.

Our approach to these topics relied on analysis of cysteine substitution mutants, as initially outlined in studies of the acetylcholine channel (*32*) and UhpT (*25*) (see also refs *13–17* and *26*). In this work, we found that the 25 positions encompassing TM5 were largely tolerant of mutagenesis (Table 1), with only four yielding nonfunctional product. Among these four, the G140 and G144 pair merits specific comment, since others have noted that the GxxxG motif is often associated with helix−helix interaction in membrane proteins (see ref *33* for a review). Positions 140 and 144 are found at the cytoplasmic end of TM5, facing the entrance of the permeation pathway in the inward-facing conformation (Figure 5B). One presumes that this end of the pathway closes as the periplasmic entrance is opened and that an effective seal would require close packing of cytoplasmic-facing surfaces, including the region containing G140 and G144. In fact, a conformational change in this area accompanies initiation of turnover (Figure 4, and see below), and it is plausible that the $G_{140}xxxG_{144}$ motif participates in this event. We also note that a similar motif ($G_{336}xxxS_{340}$) is found in a symmetrical position in the C-terminal domain on the opposite side of the pathway. This is of interest since GxxxG interaction motifs mediate hetero- and homodimerizations among the ErbB1 and ErbB2 receptors (see ref *33*), and one might view closure of the OxlT cytoplasmic entrance as a pseudodimerization event involving the homologous TM_{1-6} and TM_{7-12} domains. Similar helix−helix interactions involving the $G_{149}xxxG_{153}$ pair may also be important, since the G153C mutant was not recovered. But because the G149C derivative exhibited a 10% residual activity (Table 1),

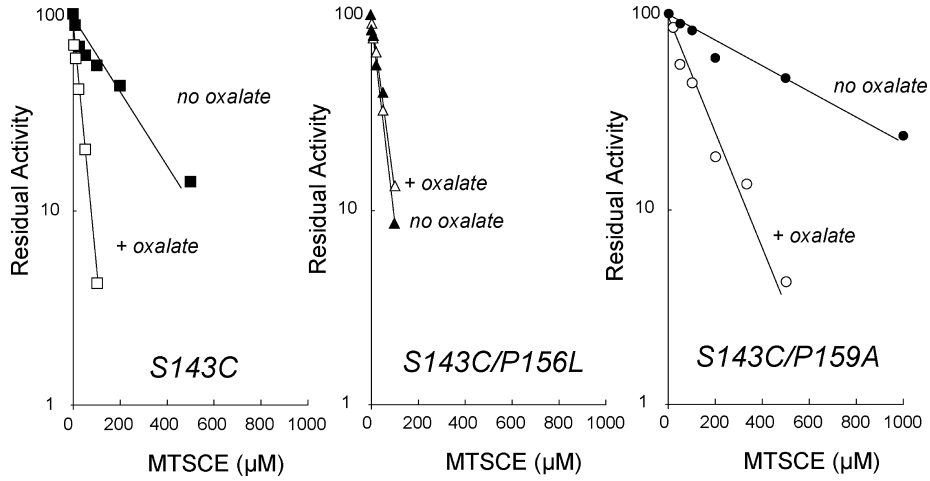

FIGURE 4: Effect of P156 on substrate-triggered sensitivity to MTSCE. MTSCE sensitivity of S143C (Figure 3) was monitored in the absence of oxalate or in the presence of 5 mM oxalate, for variants carrying the single-cysteine mutation S143C alone (left) or in combination with P156L (middle) or P159A (right). In this experiment, IC_{50} values in the absence and presence of substrate were 160 and 28 μM for S143C, 27 and 36 μM for the S143C/P156L double mutant, and 460 and 96 μM for the S143C/P159A variant, respectively.

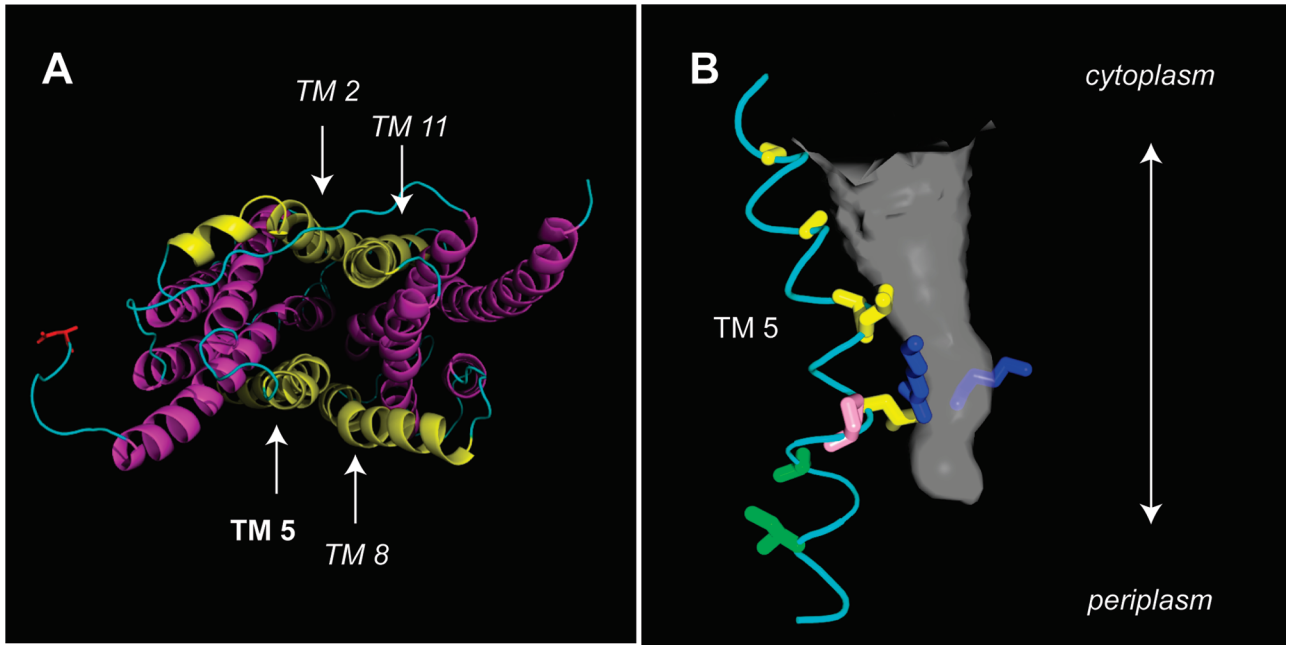

FIGURE 5: OxlT homology model. (A) Ribbon diagram depicting OxlT as viewed from the cytoplasmic surface. TM5 and its structural counterparts (TM2, TM8, and TM11) are colored yellow, while the remaining transmembrane helices are colored magenta; the N-terminus is colored red for reference. (B) Permeation pathway. The gray cone indicates that portion of the permeation pathway exposed to solvent in the OxlT inward-facing conformation, as derived from analysis using CAVER. Probe-responding residues with IC_{50} values of $\leq$300 μM (see Table 2) are colored yellow (proximal to P156) or green (distal to P156); P156 is colored pink. The substrate-binding residues, R272 and K355, are colored blue.

the argument is not as convincing. Added tests with substitutions of larger side chain volume may be helpful in this context.

Cysteine substitution mutagenesis was used to allocate residue(s) of TM5 to the permeation pathway, using operational criteria established earlier, in particular, that the residue must be accessible to hydrophilic probes from either membrane surface (*25, 26*). Use of proteoliposomes is especially helpful in such work, since after reconstitution by detergent dilution, MFS family members such as OxlT, GlpT, and UhpT are found in both inside-out and right-side-out orientations, each of which has equivalent activity (*16, 24, 34*). Accordingly, substantial inhibition ($\geq$80%) by an externally added probe reflects accessibility from both entrance and exit points of the permeation pathway. This criterion identified a number of positions as being accessible to MTS-linked probes, yielding three distinct classes of response (Table 1 and Figure 1); further study of representative examples of each class indicated in each case that MTS reactivity could be influenced by the presence of substrate, as anticipated for residues along the permeation pathway (see refs *14* and *16*).

The TM5 positions responding to MTS-linked probes are found largely in the cytoplasmic portion of the helix, extending from the cytoplasmic entrance to beyond the region of ligand binding by R272 and K355 (Figure 5B); residues in the equivalent region have also been assigned to the permeation pathway in TM2 and TM11 (*16, 17*). In TM5, the main responsive positions (S143C, A147C, G151C, and L152C, each with MTSCE IC_{50} values of

40−100 μM) face the permeation pathway visualized by the inward-facing conformation, while at the periplasmic end of TM5, the two responsive residues (L158C and I161C, with MTSCE IC_{50} values of 200−300 μM) fall on the opposite helical face (Figure 5B). The former observation is consistent with the structural analysis, but it is not possible to assess the responsiveness of the latter positions, since no example within the MFS has provided a model of the outward-facing conformation. Nevertheless, a simple interpretation of the accessibility of L158C and I161C would suggest that the transition between the inward- and outward-facing structures involves a conformational change that induces a reorientation of TM5 that exposes these two residues to the permeation pathway.

As noted earlier, work reported here supports the idea that there is a change of orientation of at least part of TM5 during substrate binding and/or transport. Thus, the presence of oxalate increases the sensitivity of the S143C variant to MTSCE (Figures 2 and 4), and we presume this is one reflection of the larger-scale reorganization that accompanies substrate binding and transport. The presence of P156, at the center of TM5, appears to be required for the observation of changes in accessibility of G143C (Figure 4), and although the mechanistic basis for this is not yet clear, two general possibilities seem feasible. For example, it has been suggested that cis−trans isomerizations of proline might drive conformational changes in membrane proteins (*27, 28*); recent thinking no longer emphasizes this (*33*) but instead points to an increased local backbone flexibility as being relevant (*35*). Alternatively, proline can play a structural role by introduction of a kink in an α-helix. In fact, OxlT TM5 has two prolines (P156 and P159) and as a result displays a distinct curvature (*13*), one that is thought to be important in guiding the rotation of the N- and C-terminal domains about the TM2−TM11 and TM5−TM8 interfaces. In the absence of P156, then, TM5 curvature may be reduced and/or its flexibility may be restricted, limiting the conformational changes at the TM5 cytoplasmic pole so that C143 displays a uniform accessibility to MTSCE. In either instance, the finding of conformational changes in TM5 remains significant in that it documents that the N-terminal TM_{1-6} domain participates in the OxlT transport cycle, reinforcing the idea that OxlT and GlpT share mechanistic as well as structural similarities and that the rocker-switch-type model is a legitimate structural basis for the alternating access characteristic of members of the MFS.

ACKNOWLEDGMENT

We thank Dr. Q. Yang for providing the OxlT homology model figures.

REFERENCES

1. Allison, M. J., Dawson, K. A., Mayberry, W. R., and Foss, J. G. (1985) *Oxalobacter formigenes* gen. nov., sp. nov.: Oxalate-degrading anaerobes that inhabit the gastrointestinal tract. *Arch. Microbiol. 141*, 1–7.
2. Anantharam, V., Allison, M. J., and Maloney, P. C. (1989) Oxalate: formate exchange. The basis for energy coupling in *Oxalobacter*. *J. Biol. Chem. 264*, 7244–7250.
3. Ruan, Z. S., Anantharam, V., Crawford, I. T., Ambudkar, S. V., Rhee, S. Y., Allison, M. J., and Maloney, P. C. (1992) Identification, purification and reconstitution of OxlT, the oxalate:formate antiport protein of *Oxalobacter formigenes*. *J. Biol. Chem. 267*, 10537–10543.
4. Maloney, P. C. (1994) Bacterial transporters. *Curr. Opin. Cell Biol. 6*, 571–582.
5. Saier, M. H., Jr., and Busch, W. (2002) The transporter classification (TC) system. *Crit. Rev. Biochem. Mol. Biol. 37*, 287–337.
6. Henderson, P. J. (1993) The 12-transmembrane helix transporters. *Curr. Opin. Cell Biol. 5*, 708–721.
7. Maiden, M. C., Davis, E. O., Baldwin, S. A., Moore, D. C., and Henderson, P. J. (1987) Mammalian and bacterial sugar transport proteins are homologous. *Nature 325*, 641–643.
8. Hirai, T., Heymann, J., Shi, D., Sarker, R. I., Maloney, P. C., and Subramaniam, S. (2002) Three-dimensional structure of a bacterial oxalate transporter. *Nat. Struct. Biol. 9*, 597–600.
9. Hirai, T., Heymann, J., Maloney, P. C., and Subramaniam, S. (2003) Structural model for 12-helix transporters belonging to the major facilitator superfamily. *J. Bacteriol. 185*, 1712–1718.
10. Abramson, J., Smirnova, I., Kasho, V., Verner, G., Kaback, H. R., and Iwata, S. (2003) Structure and mechanism of the lactose permease of *Escherichia coli*. *Science 301*, 610–615.
11. Huang, Y., Lemieux, M. J., Song, J., Auer, M., and Wang, D. N. (2003) Structure and mechanism of the glycerol-3-phosphate transporter from *Escherichia coli*. *Science 301*, 616–620.
12. Yin, Y., He, X., Szewczyk, P., Nguyen, T., and Chang, G. (2006) Structure of the multidrug transporter EmrD from *Escherichia coli*. *Science 312*, 741–744.
13. Maloney, P. C., Yang, Q., Wang, X., Ye, L., Mentrikoski, M., Mohammadi, E., and Kim, Y.-M. (2005) Experimental tests of a homology model for OxlT, the oxalate transporter of *Oxalobacter formigenes*. *Proc. Natl. Acad. Sci. U.S.A. 102*, 8513–8518.
14. Wang, X., Sarker, R. I., and Maloney, P. C. (2006) Analysis of substrate-binding elements in OxlT, the oxalate:formate antiporter of *Oxalobacter formigenes*. *Biochemistry 45*, 10344–10350.
15. Fu, D., and Maloney, P. C. (1998) Structure/function relationships in OxlT, the oxalate-formate transporter of *Oxalobacter formigenes*. Topological features of trans-membrane helix as visualized by site-directed fluorescent labeling. *J. Biol. Chem. 273*, 17962–17967.
16. Fu, D., Sarker, R. I., Abe, K., Bolton, E., and Maloney, P. C. (2001) Structure/function relationships in OxlT, the oxalate-formate transporter of *Oxalobacter formigenes*. Assignment of transmembrane helix to the translocation pathway. *J. Biol. Chem. 276*, 8753–8760.
17. Ye, L., and Maloney, P. C. (2002) Structure/function relationships in OxlT, the oxalate/formate antiporter of *Oxalobacter formigenes*: Assignment of transmembrane helix to the translocation pathway. *J. Biol. Chem. 277*, 20372–20378.
18. Abe, K., Ruan, Z.-S., and Maloney, P. C. (1996) Cloning, sequencing and expression in *Escherichia coli* of OxlT, the oxalate/formate exchange protein of *Oxalobacter formigenes*. *J. Biol. Chem. 271*, 6789–6793.
19. Fu, D., and Maloney, P. C. (1997) Evaluation of secondary structure of OxlT, the oxalate/formate transporter of *Oxalobacter formigenes*, by circular dichroism spectroscopy. *J. Biol. Chem. 272*, 2129–2135.
20. Ambudkar, S. V., and Maloney, P. C. (1986) Bacterial anion exchange. Use of osmolytes during solubilization and reconstitution of phosphate-linked antiport from *Streptococcus lactis*. *J. Biol. Chem. 261*, 10079–10086.
21. Baron, C., and Thompson, T. (1975) Solubilization of bacterial membrane proteins using alkyl glucosides and dioctanoly phosphatidylcholine. *Biochim. Biophys. Acta 382*, 276–285.
22. Racker, E., Violand, B., O'Neal, S., Alfonzo, M., and Telford, J. (1979) Reconstitution, a way of biochemical research: Some new approaches to membrane-bound enzymes. *Arch. Biochem. Biophys. 198*, 470–477.
23. Newman, M. J., and Wilson, T. H. (1980) Solubilization and reconstitution of the lactose transport system from *Escherichia coli*. *J. Biol. Chem. 255*, 10583–10586.
24. Fann, M.-C., and Maloney, P. C. (1998) Functional symmetry of UhpT, the sugar phosphate transporter of *Escherichia coli*. *J. Biol. Chem. 273*, 33735–33740.
25. Yan, R.-T., and Maloney, P. C. (1993) Identification of a residue in the translocation pathway of a membrane carrier. *Cell 75*, 37–44.
26. Yan, R.-T., and Maloney, P. C. (1995) Residues in the pathway through a membrane transporter. *Proc. Natl. Acad. Sci. U.S.A. 92*, 5973–5976.

27. Randl, C. J., and Deber, C. M. (1986) Hypothesis about the function of membrane-buried proline residues in transport proteins. *Proc. Natl. Acad. Sci. U.S.A. 83*, 917–921.
28. Williams, K. A., and Deber, C. M. (1991) Proline residues in transmembrane helices: Structural or dynamic role? *Biochemistry 30*, 8919–8923.
29. Fann, M.-C., Davies, A. H., Varadhachary, A., Kuroda, T., Sevier, C., Tsuchiya, T., and Maloney, P. D. (1998) Identification of two essential arginine residues in UhpT, the sugar phosphate antiporter of *Escherichia coli*. *J. Membr. Biol. 164*, 187–195.
30. Lemieux, M. J., Huang, Y., and Wang, D. N. (2004) The structural basis of substrate translocation by the *Escherichia coli* glycerol-3-phosphate transporter: A member of the major facilitator superfamily. *Curr. Opin. Struct. Biol. 14*, 405–412.
31. Law, C. J., Yang, Q., Soudant, C., Maloney, P. C., and Wang, D.-N. (2007) Kinetic evidence is consistent with the rocker-switch mechanism of membrane transport by GlpT. *Biochemistry 46*, 12190–12197.
32. Akabas, M. H., Stauffer, D. A., Xu, M., and Karlin, A. (1992) Acetylcholine receptor channel structure probed in cysteine-substitution mutants. *Science 258*, 307–310.
33. Senes, A., Engel, D. E., and DeGrado, W. F. (2004) Folding of helical membrane proteins: The role of polar, GxxxG-like and proline motifs. *Curr. Opin. Struct. Biol. 4*, 465–479.
34. Fann, M.-C., Busch, A., and Maloney, P. C. (2003) Functional characterization of cysteine residues in GlpT, the glycerol 3-phosphate transporter of *Escherichia coli*. *J. Bacteriol. 185*, 3863–3870.
35. Tieleman, D. P., Shrivastava, I. H., Ulmschneider, M. R., and Sansom, M. S. (2001) Proline-induced hinges in transmembrane helices: Possible roles in ion channel gating. *Proteins 44*, 63–72.

BI8001314